

Projected Development of COVID-19 in Louisiana

Ka-Ming Tam,^{1,2} Nicholas Walker,¹ and Juana Moreno^{1,2}

¹*Department of Physics & Astronomy, Louisiana State University, Baton Rouge, Louisiana 70803, USA*

²*Center for Computation & Technology, Louisiana State University, Baton Rouge, Louisiana 70803, USA*

(Dated: January 20, 2022)

At the time of writing, Louisiana has the third highest COVID-19 infection per capita in the United States. The state government issued a stay-at-home order effective March 23rd. We analyze the projected spread of COVID-19 in Louisiana without including the effects of the stay-at-home order. We predict that a large fraction of the state population would be infected without the mitigation efforts, and would certainly overwhelm the capacity of Louisiana health care system. We further predict the outcomes with different degrees of reduction in the infection rate. More than 70% of reduction is required to cap the number of infected to under one million.

I. INTRODUCTION

The identification and verification of human-to-human transmission of the coronavirus disease (COVID-19) in early January of 2020 in Wuhan, China triggered the start of a worldwide pandemic. As of April 5, there are more than 1.2 million confirmed cases and more than 67,000 deaths attributed to COVID-19. The first case in the US was confirmed in Washington State on January 20. The number of reported cases until early March was rather low. The exceedingly slow spreading rate in these early months may be partially due to the lack of adequate testing, which remains a major issue at the time of writing. The cases dramatically increased in the USA in early March, with most cases in the states of Washington, New York, and California. It was not until March 9 that the first case in Louisiana was identified.

The growth rate of infections in Louisiana has been alarming since the confirmation of the first case. Louisiana state government responded swiftly by closing all K-12 public schools on March 13. On March 16, public gatherings of more than 50 people were prohibited, and bars, bowling alleys, casinos, fitness facilities, and movie theaters were closed. Furthermore, a stay-at-home order was issued on March 23.

Adequate testing for COVID-19 remains limited in the USA. For this reason, accurately predicting the trajectory of the spread of COVID-19 by relying on the number of confirmed cases alone is a rather questionable approach. While the Susceptible-Infected-Recovered (SIR) model may well describe the dynamics of the spreading^{1,2}, accurate predictions rely on knowing the number of confirmed cases, which is severely hampered by the limitations of testing. This is particularly significant in the early stages of the spread of the disease when the percentage of people tested is very small, and the spread by infected people who are asymptomatic is very significant.

Alternatively, the number of fatalities attributed to COVID-19 may be a more reliable parameter for tracing the dynamics of the virus spread. Combining this information with the mortality rate can be a better strategy to predict the number of cases than relying on the con-

firmed infection count alone. The goal of this paper is to extract the dynamics of COVID-19 in Louisiana from the data of the death count supplemented with the confirmed cases. We then run several scenarios with different reduction of the infection rate and calculate the number of people infected in each case. We conclude with suggestions to improve the model and, as consequence, its predictions.

II. MODEL

Our model is based on the Susceptible-Infected-Recovered (SIR) model³⁻³² with the modification of including the number of quarantined people (Q), as has been considered elsewhere.³⁻⁵ The equations defining the model are the following:

$$\frac{dS(t)}{dt} = -\beta \frac{S(t)I(t)}{N}, \quad (1)$$

$$\frac{dI(t)}{dt} = \beta \frac{S(t)I(t)}{N} - (\alpha + \eta)I(t), \quad (2)$$

$$\frac{dQ(t)}{dt} = \eta I(t) - \gamma Q(t), \quad (3)$$

$$\frac{dR(t)}{dt} = \gamma Q(t) + \alpha I(t), \quad (4)$$

where N is the total population size, S is the susceptible population count, I is the unidentified infected population count, Q is the number of identified cases, and R includes the number of recovered and dead patients. The model is characterized by the following parameters: β is the infection rate, η is the detection rate, α is the recovery rate of asymptomatic people, and γ includes the recovery rate and the casualty rate of the quarantined patients. This model is equivalent to the standard SIR model if we are not interested into differentiating between Q and R .

We further assume that the rate of increase in the number of casualties is proportional to the number of infected at the early stage of the epidemic,

$$\frac{dC(t)}{dt} = \delta I(t), \quad (5)$$

where δ is the mortality rate. This is a good approximation at the beginning of the virus spread when the number of quarantined patients is a small percentage of the total population. This equation is not combined in any way with Eq. 1-4, it is only used to estimate the model parameters at the start of the epidemic.

III. ANALYSIS

We first consider Eq. 2, assuming the susceptible population count is very close to that of the total population, $S \sim N$, which is justifiable at the beginning of the epidemic since only a small fraction of the population is infected. With this assumption one can decouple the infected population count from the other parameters to obtain:^{3,5}

$$I(t) = I(0) \exp [(\beta - (\alpha + \eta))t]. \quad (6)$$

Solving Eq. 5, the casualty count as a function of time can be written as

$$C(t) = \frac{\delta I(0)}{\beta - (\alpha + \eta)} \exp [(\beta - (\alpha + \eta))t]. \quad (7)$$

The exponential growth of the number of fatalities at the beginning of the epidemic should represent the spreading of COVID-19 reasonably well since the mechanisms for slowing the dynamics, such as improved detection and social distancing, are delayed in time

By fitting the available fatalities data (see Appendix) between March 14 and 31 to Eq. 7, the parameters of the model can be determined. Fig. 1 displays the fit which provides an estimate of $C(t) \approx 5.04 \exp [0.228t]$. The dynamics (exponent) is thus given as $\beta - (\alpha + \eta) = 0.228$. From the value of the exponent we can estimate the time for doubling the casualties count: $\ln(2)/0.228 \approx 3.04$ days. Moreover, the proportionality constant can be used to estimate the initial number of infections $I(0)$ if the mortality rate δ is known.

The mortality rate is estimated by combining the accumulated mortality rate data and the median time between infection and death. It is estimated that the median time between infection and the onset of symptoms is about five days, while the median time between the onset of symptoms and death is eight days.³³⁻³⁶ It is worth noting that the distribution of these time periods is close to a log-normal, thus a more sophisticated analysis should include the effects of the non-self-averaging behavior of the distribution. Only the median values are used in the present work.

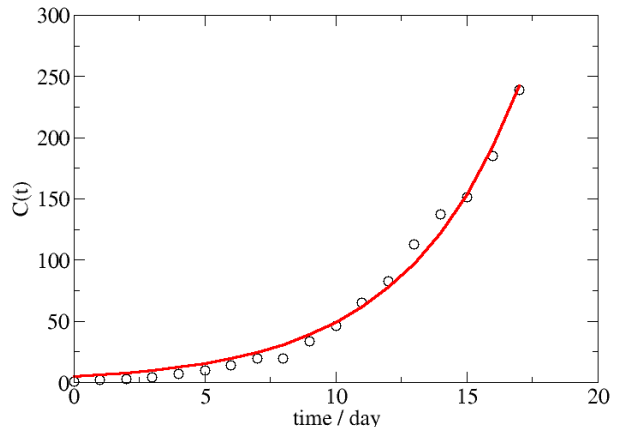


FIG. 1: COVID-19 casualties in Louisiana, $C(t)$, as a function of time with March 14 as day 0, data is represented by circles. The parameters of Eq. 7 are fit to the data, providing an approximation to the number of deaths as a function of time: $C(t) \approx 5.04 \exp [0.228t]$.

The accumulated mortality rate is estimated to be 2.3%³⁷. Notably, the mortality rate does indeed vary by region. This may be due to the rate of testing as well as the capacity of health care facilities. For areas in which health care facilities have been overrun, the death rate would be much higher. Notwithstanding these uncertainties, assuming that the health care facilities have not yet been overrun, the mortality rate is estimated to be $\delta \approx \frac{0.023}{5+8} \approx 0.0018$. This also provides an estimation of the number of persons who carries the virus but not detected at day 0, $I(0)$, which is given as $I(0) \approx \frac{5.04}{\delta} \times 0.228 \approx 650$. This reveals that even as early as March 14, the number of infected people is already at the order of hundreds.

Now we consider the number of confirmed cases at the start of the epidemic, $P(t)$. This is given by the sum of $Q(t)$ and $R(t)$ subtracted by the number of persons who recovered without being tested. The rate of change on the number of reported cases can be obtained by combining Eqs. 3 and 4 and subtracting $\alpha I(t)$:

$$\frac{dP(t)}{dt} = \eta I(t) \quad (8)$$

with $I(t)$ given by Eq. 6, we obtain:^{3,5}

$$P(t) \approx \frac{\eta}{\beta - \alpha - \eta} I(0) \exp [0.228t]. \quad (9)$$

By fitting the number of confirmed cases (Fig.2) we find $P(t) \approx 117 \exp [0.228t]$, which provides the estimate $\frac{\eta}{\beta - \alpha - \eta} I(0) \approx 117$. Since $I(0)$ and $(\beta - \alpha - \eta)$ are known from fitting to the number of casualties, we find

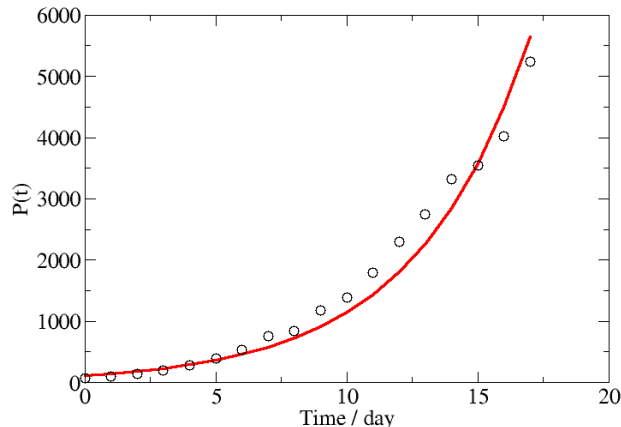


FIG. 2: The number of confirmed cases of COVID-19 in Louisiana, $P(t)$, as a function of time with March 14 as day 0. The data is represented by circles, the red line is the best fit, $P(t) \approx 117 \exp[0.228t]$. Note, we only fit the coefficient in front, the exponent is given by from the death count, see fig. 1.

$\eta \approx 117 \times \frac{0.228}{650} \approx 0.041$. There remains one parameter to be determined, the recovery rate of asymptomatic people, α . Assuming that the average time or recovery or dead are both 13 days, and half of the infected never show any symptoms thus they are not been tested³⁹. We can estimate $\alpha = 0.5/13 \approx 0.0385$. This is probably the upper bound of the estimate, in reality this could be smaller. This additionally provides the value for β as 0.307.

With these parameters, Eqs. 1-4 can be solved and used to predict the spread of the disease. Fig. 3 displays the time evolution of the number of unidentified persons who carry the virus, $I(t)$, the number of persons who are either in quarantine or recovered, $Q(t) + R(t)$, and the total number of persons who have ever been infected, $Q(t) + R(t) + I(t)$. The number of infections but unidentified, $I(t)$, grows exponentially, as expected from Eq. 6, at the initial stage, and this behavior continues until about day 25, when around 100,000 people are infectious. The exponent of ~ 0.228 suggests the number of cases double approximately every three days, which seems to be consistent with the data in many areas of the world before the mitigation efforts are kicked in. After day 25, the rate of increase slow down due to the combination of the decrease on the number of susceptible (uninfected) people and the increase on the number of recoveries. The number of infected cases ceases to grow exponentially, but rather becomes a stable but constant increases until peaking at around day 50, corresponding to early May. On the other hand, the number of quarantined and recovered people resembles a logistic function.

To compare with other states which already have widespread epidemic, we use the described method to calculate the infection rate (β), the testing rate (η), and

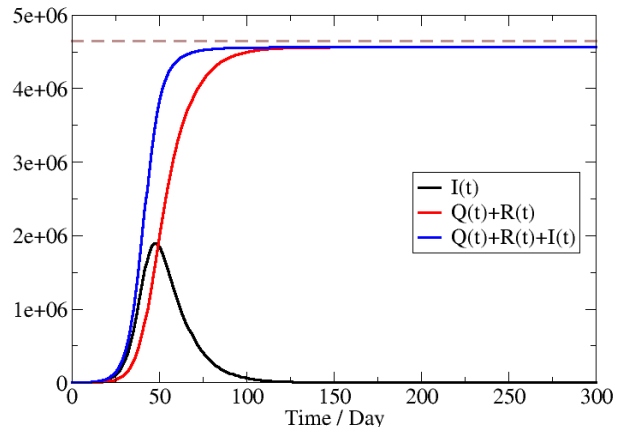


FIG. 3: The number of unidentified but infected people, $I(t)$, the number of quarantined and recovered people, $Q(t)+R(t)$, and the number of people who are ever infected, $Q(t)+R(t)+I(t)$, as a function of time since March 14. Horizontal dashed line at the total population of Louisiana, 4.65 million.

State	$\beta - \alpha - \eta$	η	R_0
Louisiana	0.228	0.041	3.87
Florida	0.198	0.114	2.30
Georgia	0.161	0.054	3.74
Texas	0.206	0.114	2.35
California	0.205	0.083	3.69
Illinois	0.237	0.085	2.92
New Jersey	0.287	0.079	3.44
New York	0.231	0.070	3.13

TABLE I: Table of the value of $\beta - \alpha - \eta$, η , and R_0 for different states. Note that the reproduction number, R_0 , is in line with the other studies³⁸.

the reproduction number ($R_0 = \beta/(\eta + \alpha)$) of selected states. Result are displayed in Table I. Note than the reproduction number of Louisiana is the highest among the states listed in the table.

Within the present model, there are two major routes to slow the initial exponential growth of the epidemic, which is characterized by the parameter $\beta - (\alpha + \eta)$. The first one is to decrease the infection rate, β . The second route is to increase the testing rate, η . To increase the recovery rate from unidentified persons, α , can also reduce the spread, but it is unlikely to be achieved. As the stay-at-home order was issued on March 23, it is expected that the infection rate should be drastically reduced. We simulate new scenarios with the assumption that social contact is reduced so that the infection rate decreases by

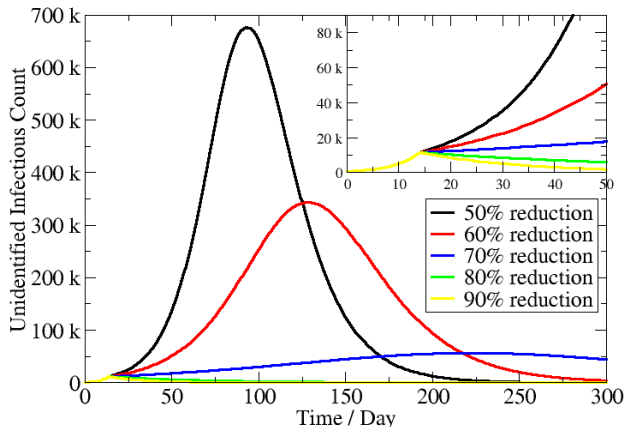


FIG. 4: The number of people who are infected and carrying the virus without being identified, $I(t)$, as a function of time, with March 14 as day 0. We assume the mitigation efforts reduce the infection rate by 50 %, 60%, 70%, 80%, and 90% from day 15 (6 days after the stay-at-home order), and the sum of the testing rate and recovery rate of asymptomatic people remains unchanged. The inset is a zoom for the first 50 days.

50%, 60%, 70%, 80%, and 90% starting at day 15. The results are shown in Fig. 4 and 5.

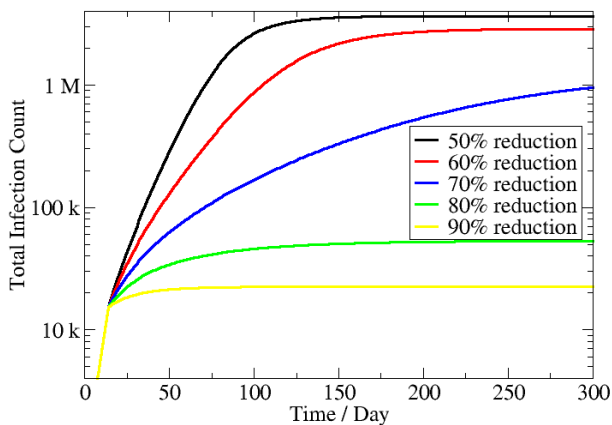


FIG. 5: The number of people who are ever infected the virus (log scale), $I(t) + Q(t) + R(t)$, as a function of time, with March 14 as day 0. We assume the mitigation efforts reduce the infection rate by 50 %, 60%, 70%, 80%, and 90% from day 15, and the sum of the testing rate and recovery rate of asymptomatic people remains unchanged.

We find that there is a substantial drop of the active virus carriers even with a 50% reduction in the infection rate. However, the number of people who will be infected

still exceeds one million if the reduction in the infection rate is smaller than 70%. This suggests the importance of strict measures in social distancing. Perhaps it also suggests the importance of wearing basic protective gear to further reduce the infection rate.

IV. DISCUSSION

There are many uncertainties in this simplified model which can be improved over time as more data become available. Improvement can be achieved by including additional factors, such as correlation with different age groups, correlation with the health condition of the population, the availability of public health care, the effect of higher ambient temperature and humidity, and many others. Some of those factors are likely beyond the SIR model which implicitly assume that the population is homogeneous and well mixed, and that infection occurs without time delay. However, given the rather limited data available today, it is not clear that more sophisticated models may provide much better predictions.

In spite of the rather simple model being employed in this analysis, it provides a baseline for the spread of the COVID-19 in Louisiana in the absence of mitigation efforts. The situation is clearly dire, as a very large fraction of the population will get infected with a peak on the number of infections around early May.

With the current mitigation efforts, we expect the infection rate will be greatly reduced. Currently, we do not have data to support the effectiveness of current mitigation efforts as the trend still fits rather well to the initial stage of exponential growth.

The main projection from this work is that more than 70% of reduction in the infection rate is needed to keep the infected count below one million. Increasing testing capacity and providing protective gear to further reduce the infection rate seem to be reasonable measures.

V. ACKNOWLEDGMENT

This work is funded by the NSF EPSCoR CIMM project under award OIA-1541079. This work used the high performance computational resources provided by the Louisiana Optical Network Initiative (<http://www.loni.org>) and HPC@LSU computing. Additional support (KMT) was provided by NSF Materials Theory grant DMR-1728457 and NSF Office of Advanced Cyberinfrastructure grant OAC-1931445.

VI. APPENDIX

Number of people tested for COVID-19, people confirmed infected, and the resulting casualty count in Louisiana from March 14 to March 31 are shown in the Table II⁴⁰⁻⁴²

Date	Tested	Confirmed	Death
Mar 14	210	77	1
Mar 15	247	103	2
Mar 16	374	136	3
Mar 17	531	196	4
Mar 18	703	280	7
Mar 19	899	392	10
Mar 20	1,931	537	14
Mar 21	3,302	763	20
Mar 22	3,498	837	20
Mar 23	5,948	1,172	34
Mar 24	8,603	1,388	46
Mar 25	11,451	1,795	65
Mar 26	18,299	2,305	83
Mar 27	21,359	2,746	119
Mar 28	25,161	3,315	137
Mar 29	27,871	3,540	151
Mar 30	34,033	4,025	185
Mar 31	38,967	5,237	239

TABLE II: Number of test conducted, number of confirmed cases, and number of death from Mar 14 to Mar 31 from COVID-19 in Louisiana.

-
- ¹ A. Huppert and G. Katriel, *Clin. Microbiol. Infect.* 19, 999 (2003).
- ² W. O. Kermack and A. G. McKendrick, *Proc. R. Soc. Lond.*, 115, 700 (1927).
- ³ C. Crokidakis, arXiv:2003.12150.
- ⁴ M. Bin, P. Cheung, E. Crisostomi, P. Ferraro, C. Myant, T. Parisini, and R. Shorten, arXiv:2003.09930.
- ⁵ M. G. Pedersen and M. Meneghini, DOI: 10.13140/RG.2.2.11753.85600.
- ⁶ G. C. Calafiore, C. Novara, and C. Possieri, arXiv:2003.14391.
- ⁷ S. B. Bastos and D. O. Cajueiro, arXiv:2003.14288.
- ⁸ G. Gaeta, arXiv:2003.14102.
- ⁹ G. Gaeta, arXiv:2003.14098.
- ¹⁰ M. te Vrugt, J. Bickmann, and R. Wittkowski, arXiv:2003.13967.
- ¹¹ R. A. Schulz, C. H. Coimbra-Arajo, and S. W. S. Costiche, arXiv:2003.13932.
- ¹² Y. Zhang, X. Yu, H. Sun, Geoffrey R. Tick, W. Wei, and B. Jin, arXiv:2003.13901.
- ¹³ L. Dell'Anna, arXiv:2003.13571.
- ¹⁴ G. Sonnino, arXiv:2003.13540.
- ¹⁵ A. Notari, arXiv:2003.12471.
- ¹⁶ J. E. Amaro, arXiv:2003.13747.
- ¹⁷ A. Simha, R. V. Prasad, and S. Narayana, arXiv:2003.11920.
- ¹⁸ P. H. Acioli, arXiv:2003.11449.
- ¹⁹ F. Zullo, arXiv:2003.11363.
- ²⁰ R. Sameni, arXiv:2003.11371.
- ²¹ A. Radulescu and K. Cavanagh, arXiv:2003.11150.
- ²² L. Roques, E. Klein, J. Papaix, and S. Soubeyrand, arXiv:2003.10720.
- ²³ P. Teles, arXiv:2003.10047.
- ²⁴ E. L. Piccolomini and F. Zama, arXiv:2003.09909.
- ²⁵ L. Brugnano and F. Iavernaro, arXiv:2003.09875.
- ²⁶ G. Giordano, F. Blanchini, R. Bruno, P. Colaneri, A. Di Filippo, A. Di Matteo, and M. Colaneri, the COVID19 IRCCS San Matteo Pavia Task Force, arXiv:2003.09861.
- ²⁷ V. Zlatić, I. Barjašć, A. Kadović, H. Štefančić, and A. Gabrielli, arXiv:2003.08479.
- ²⁸ R. Baker, arXiv:2003.08285.
- ²⁹ K. Biswas, A. Khaleque, and P. Sen, arXiv:2003.07063.
- ³⁰ J. Zhang, L. Wang, and J. Wang, arXiv:2003.06419.
- ³¹ Y.-C. Chen, P.-E. Lu, C.-S. Chang, and T.-H. Liu, arXiv:2003.00122.
- ³² A. L. Lloyd, *Theor. Popul. Biol.*, 60, 59 (2001).
- ³³ Q. Li, X. Guan, P. Wu, et al., *N. Engl. J. Med.* 382, 1199 (2020).
- ³⁴ R. M. Anderson H. Heesterbeek, D. Klinkenberg, and T. D. Hollingsworth, *Lancet* 395, 931 (2020).
- ³⁵ WHO. Coronavirus disease (COVID2019) situation report-30.
- ³⁶ N. M. Linton, T. Kobayashi, Y. Yang, K. Hayashi, A. R. Akhmetzhanov, S.-M. Jung, B. Yuan, R. Kinoshita, and H. Nishiura, *J. Clin. Med.* 9(2), 538 (2020).
- ³⁷ Z. Wu and J. M. McGoogan, *JAMA*. doi:10.1001/jama.2020.2648.
- ³⁸ <https://www.imperial.ac.uk/mrc-global-infectious-disease-analysis/covid-19/>
- ³⁹ K. Mizumoto, K. Kagaya, A. Zarebski, and G. Chowell, *EuroSurveill* 25, 10 (2020).
- ⁴⁰ <http://ldh.la.gov/Coronavirus/>

⁴¹ https://en.wikipedia.org/wiki/2020_coronavirus_pandemic_in_Louisiana

⁴² The Advocate, <https://www.theadvocate.com/>